Ladder-like [CrCu] coordination polymers containing unique bridging modes of [Cr(C2O4)3]3− and Cr2O72−

Kanižaj, Lidija; Molčanov, Krešimir; Torić, Filip; Pajić, Damir; Lončarić, Ivor; Šantić, Ana; Jurić, Marijana

Source / Izvornik: **Dalton Transactions, 2019, 48, 7891 - 7898**

Journal article, Accepted version
Rad u časopisu, Završna verzija rukopisa prihvaćena za objavljivanje (postprint)

https://doi.org/10.1039/C9DT01195A

Dalton
Transactions

Accepted Manuscript

This article can be cited before page numbers have been issued, to do this please use: L. Kanižaj, K. Molcanov, F. Tori, D. Paji, I. Lonari, A. Šanti and M. Juric, *Dalton Trans.*, 2019, DOI: 10.1039/C9DT01195A.

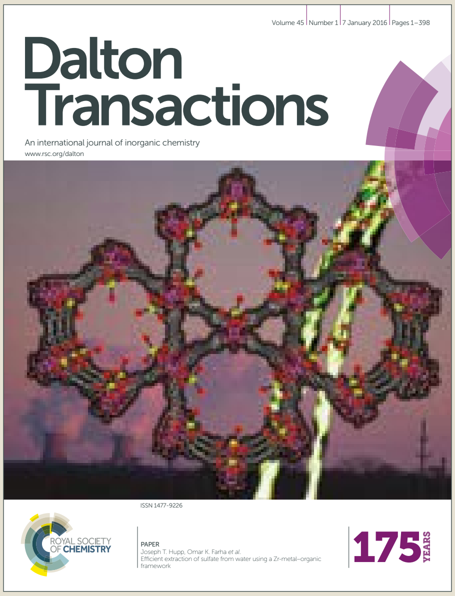

ROYAL SOCIETY
OF CHEMISTRY

rsc.li/dalton

Table of Contents

View Article Online
DOI: 10.1039/C9DT01195A

The ladder-like [CrCu] coordination polymers containing unique bridging modes of $[Cr(C_2O_4)_3]^{3-}$ and $Cr_2O_7^{2-}$

Lidija Kanižaj, Krešimir Molčanov, Filip Torić, Damir Pajić,
Ivor Lončarić, Ana Šantić and Marijana Jurić

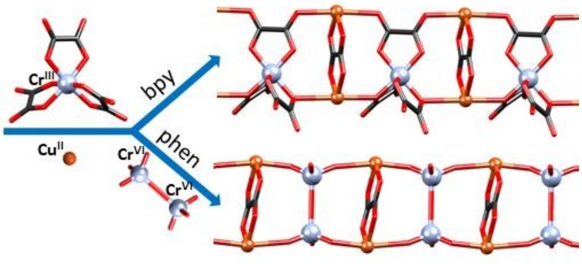

Three coordination polymers having ladder-like topologies owing to novel and unique bridging modes of $[Cr(C_2O_4)_3]^{3-}$ or $Cr_2O_7^{2-}$ show strong antiferromagnetic interaction between copper(II) ions through oxalate bridge: $\{A[CrCu_2(bpy)_2(C_2O_4)_4]\cdot H_2O\}_n$ [A = K^+ (**1**) and NH_4^+ (**2**); bpy = 2,2′-bipyridine] and $[(Cr_2O_7)Cu_2(C_2O_4)(phen)_2]_n$ (**3**; phen = 1,10-phenanthroline).

View Article Online
DOI: 10.1039/C9DT01195A

Journal Name

ARTICLE

The ladder-like [CrCu] coordination polymers containing unique bridging modes of $[Cr(C_2O_4)_3]^{3-}$ and $Cr_2O_7^{2-}$

Received 00th January 20xx,
Accepted 00th January 20xx

DOI: 10.1039/x0xx00000x

www.rsc.org/

Lidija Kanižaj,[a] Krešimir Molčanov,[a] Filip Torić,[b] Damir Pajić,[b] Ivor Lončarić,[a] Ana Šantić[a] and Marijana Jurić[a]*

Three heterometallic one-dimensional (1D) coordination polymers $\{A[CrCu_2(bpy)_2(C_2O_4)_4]\cdot H_2O\}_n$ [A = K^+ (**1**) and NH_4^+ (**2**); bpy = 2,2′-bipyridine] and $[(Cr_2O_7)Cu_2(C_2O_4)(phen)_2]_n$ (**3**; phen = 1,10-phenanthroline) with interesting topology have been synthesized using a building block approach and characterized by single-crystal X-ray diffraction, IR and impedance spectroscopy, magnetization measurements, and DFT calculations. Due to the partial decomposition of the building block $[Cr(C_2O_4)_3]^{3-}$, all three compounds contain oxalate-bridged $[Cu_2(L)_2(\mu\text{-}C_2O_4)]^{2+}$ units [L = bpy (**1** and **2**) and phen (**3**)]. In compounds **1** and **2** these cations are mutually connected through oxalate groups from $[Cr(C_2O_4)_3]^{3-}$, thus forming ladder-like topologies. Unusually, three different bridging modes of the oxalate ligand are observed in these chains. In compound **3** copper(II) ions from cationic units are bridged through oxygen atoms of $Cr_2O_7^{2-}$ anions in a novel ladder-like mode. Very strong antiferromagnetic coupling observed in all three compounds, determined from magnetization measurements and confirmed by DFT calculations (J = –343, –371 and –340 cm^{-1} for **1**, **2** and **3**, respectively), appears between two copper(II) ions interacting through oxalate bridge.

Introduction

Coordination polymers (CPs) have been extensively studied due to a large variety of topologies and structures leading to a diverse platform of physical and chemical properties, which makes them prototypes of multifunctional molecular materials.[1] In this context, the oxalate-based compounds of various transition metals have been the subject of numerous studies; the oxalate moiety, $C_2O_4^{2-}$, acts as a linker between metal centres, with various possibilities of coordination to metal centres yielding open structures with dimensionalities ranging from zero to three. A property of oxalate ions that has been of specific interest is their ability to mediate electronic effects between paramagnetic metal ions. A facile approach for the preparation of (hetero)polynuclear species with predetermined structures and spin topologies, known as “complexes as ligands” or “building-block chemistry”, involves the use of anionic mononuclear complexes as ligands in reaction with a second metal ion. In particular, the tris(oxalato)metalate anions $[M(C_2O_4)_3]^{3-}$ (M = trivalent metal) have been widely used as ligands toward (paramagnetic) metal ions in the preparation mostly of two- (2D) and three-dimensional (3D) extended systems of a general formula $[M_a^{II}/^{III}M_b^{I}/^{II}(C_2O_4)]_n^{2n-/n-}$. These anionic networks provide magnetic properties and are able to host various functional cations, paving the way to a rational synthesis of magnetic multifunctional materials.[1–3]

Also, it is well known, that large metal-oxo anions, such as $Cr_2O_7^{2-}$consisting of two apex-linked distorted tetrahedral, provide construction of novel heterometallic systems. Whereas many structural studies of simple dichromates have been reported, the use of the dichromate anion as a bridging ligand forming multi-dimensional networks is not explored so deeply.[4]

Beside heterometallic $[Cr^{III}Cu^{II}]$ oxalate-based CPs prepared using $[Cr(C_2O_4)_3]^{3-}$, we have started to design so far unexplored hybrid polymers of copper(II) prepared using two building blocks of chromium, $[Cr(C_2O_4)_3]^{3-}$ and $Cr_2O_7^{2-}$. Mostly, oxalate groups from $[Cr(C_2O_4)_3]^{3-}$ act as bidentate or monodentate[2a,5,6] while $Cr_2O_7^{2-}$ acts as a bis(monodentate) bridging ligand towards other transition metals.[7–9]

In this article we report preparation and characterization of one-dimensional (1D) ladder-like heterometallic CPs: oxalate-bridged $\{A[CrCu_2(bpy)_2(C_2O_4)_4]\cdot H_2O\}_n$ [A = K^+ (**1**) and NH_4^+ (**2**); bpy =2,2′-bipyridine] obtained using $[Cr(C_2O_4)_3]^{3-}$ as building block, and oxalate- and dichromate-bridged $[(Cr_2O_7)Cu_2(C_2O_4)(phen)_2]_n$ (**3**; phen = 1,10-phenanthroline) prepared by utilizing initial block with the addition of $Cr_2O_7^{2-}$. In addition to the single-crystal diffraction, IR and impedance spectroscopy, and measurements on a SQUID magnetometer,

---

[a] *Ruđer Bošković Institute, Bijenička cesta 54, 10000 Zagreb, Croatia. E-mail: Marijana.Juric@irb.hr*

[b] *Department of Physics, Faculty of Science, University of Zagreb, Bijenička cesta 32, 10000 Zagreb, Croatia.*

† Electronic supplementary information (ESI) available: selected bond distances and angles for **1**–**3** (Table S1), molecular structures with the atom-numbering scheme of **1** and **2** (Fig. S1), topological representation of **1**–**3** (Fig. S2), disorder of dichromate moieties in **3** (Fig. S3), hydrogen bonding patterns and geometry of **1** and **2** (Fig. S4, Table S2), aromatic stacking interactions of **3** (Table S3), impedance plot of **2** (Fig. S5), the *M(H)* curves for **1**–**3** (Figs. S6–S8), selected magneto-structural parameters (Table S4). CCDC 1896153–1896155. For ESI and crystallographic data in CIF or other electronic format see DOI: 10.1039/x0xx00000x

View Article Online
DOI: 10.1039/C9DT01185A

characterization of three novel [CrCu] coordination polymers has been accomplished by means of DFT calculations.

Results and discussion

Synthesis and crystal structure of compounds 1–3

Applying the layering technique, the blue-green rod-like crystals of poorly water-soluble compounds **1** and **2** were grown from the reaction of an aqueous solution of $A_3[Cr(C_2O_4)_3]\cdot nH_2O$ (A = K^+ or NH_4^+) and methanol solution of $CuCl_2\cdot 2H_2O$ and bpy, in the molar ratio of 1 : 1 : 1. The X-ray diffraction measurements for isostructural compounds **1** and **2** crystallizing in a triclinic $P\bar{1}$ space group were performed at 293(2) K (the unit cell parameters of **1** and **2** did not show significant changes at low temperature). Structural analysis has showed that these compounds contain oxalate-bridged $[Cu(bpy)(\mu\text{-}C_2O_4)Cu(bpy)]^{2+}$ units mutually connected through oxalate groups from $[Cr(C_2O_4)_3]^{3-}$, forming 1D ladder-like $[Cr^{III}Cu^{II}]$ chains along the *a* axis (Fig. 1a, Figs. S1 and S2†). Due to the partial decomposition of the tris(oxalato)chromate(III) anion and the release of oxalate ligand from the coordination sphere of chromium(III) during the crystallization process of **1** and **2**,[10] which was consequently coordinated to copper(II) ions in reaction mixture, oxalate-bridged dinuclear $[Cu(L)(\mu\text{-}C_2O_4)Cu(L)]^{2+}$ cationic species [L = bpy (**1** and **2**) and phen (**3**)] have been further bridged yielding ladder-like chains. This appearance is not usually observed for the tris(oxalato)chromate(III) precursor, although studied compounds are prepared under mild reaction conditions, such as slightly acidic pH and room temperature. Also unusually, simple counterions K^+ and NH_4^+ from the precursors, which usually favour dissolution of tris(oxalato)metalate(III) salts, also appear as template cations in the investigated complexes **1** and **2**.

The ladder-like chains are mutually connected along *b* axis through K^+ ions as shown in Fig. 1b (the coordination sphere of K atom includes seven O atoms, six from three oxalate groups and one from water molecule of crystallization; Fig. 1c) in **1** or through hydrogen bonds of oxalate groups and NH_4^+ cations (Fig. 1d; Table S2†), forming 2D arrangement. Further, hydrogen-bonding pattern with water molecules in *c* direction in both compounds connects this layer into a 3D network (Fig. S4† and Table S2†).

Each copper(II) atom from the asymmetric complex cation $[Cu_2(bpy)_2(\mu\text{-}C_2O_4)]^{2+}$ in **1** and **2** displays elongated octahedral coordination, involving two N atoms from bpy molecule [1.958(3)–1.988(4) Å] and two O atoms from bridging bis(bidentate) oxalate group in the basal plane [1.9596(19)–1.989(3) Å], together with O atoms from the oxalate groups of the $[Cr(C_2O_4)_3]^{3-}$ anion in the apical positions (Fig. 1a; Table S1†). The O atoms in these axial positions of the coordination sphere of Cu1 are at the same time coordinated to chromium(III) atoms [Cu1–O1 = 2.760(3) and 2.7166(19) Å and Cu1–O10^i = 2.602(4) and 2.6351(19) Å for **1** and **2**, respectively; symmetry operator: (*i*) 1 + *x*, *y*, *z;* Table S1†], creating μ-1,1,2 mode of coordination of oxalate group.[11,12] Terminal O atoms of the oxalate groups of two neighboring $[Cr(C_2O_4)_3]^{3-}$ units make axial positions of the Cu2 environment [Cu2–O7 = 2.465(4) and 2.471(2) Å and Cu2–O8^i = 2.597(4) and 2.584(2) Å; for **1** and **2**, respectively; symmetry operator (*i*) 1 + *x*, *y*, *z*], thus enabling generation of μ_3-1,2,3,4 bridging oxalate mode.[13] The observed axial Cu–O distances for both compounds (on average 2.678 Å for μ-1,1,2 and 2.529 Å for μ_3-1,2,3,4) are significantly longer than the typical Cu–O covalent bonds (1.98 Å),[4] but they are considerably shorter than the sum of the van der Waals radii (2.92 Å).[14] The Cu1···Cu2 separations across the oxalate bridge in **1** and **2** are 5.1392(14) and 5.1350(6) Å, respectively; intramolecular Cr1···Cu1 distances through the oxygen atom of μ-oxalate group are 4.733(5) and 4.698(3) Å [directly 4.251(3) and 4.2242(6) Å], while Cr1···Cu2 is 6.936(9) and 6.9475(19) Å through the part of μ_3-oxalate ligand [5.399(2) and 5.4098(6) Å through space], respectively. The chromium(III) ion from $[Cr(C_2O_4)_3]^{3-}$ displays an approximately octahedral coordination geometry, involving six oxygen atoms from three bidentate oxalate groups. The values of the Cr–O bond lengths are in relatively good agreement with literature data.[4,5d] Selected bond distances and angles are given in Table S1†.

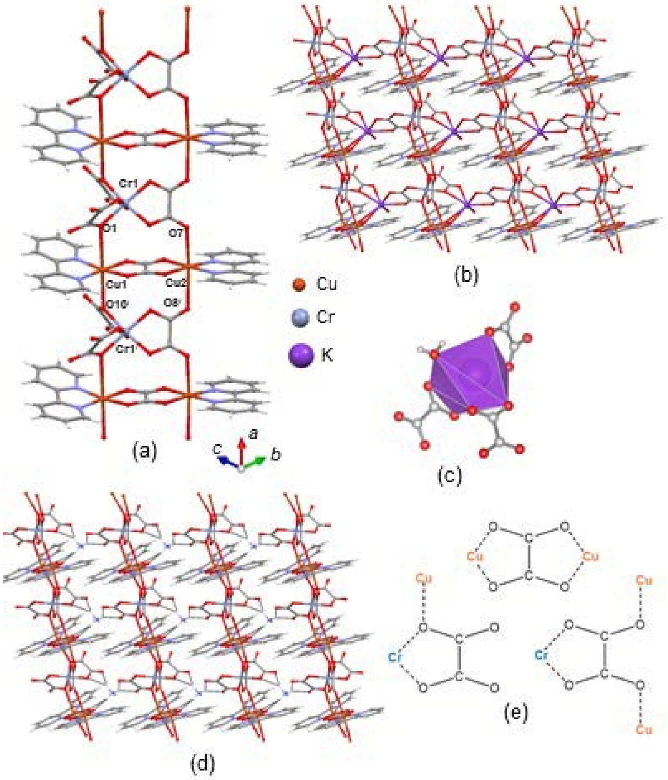

Fig. 1 (a) An 1D ladder-like chain made of $[CrCu_2(bpy)_2(C_2O_4)_4]^-$ units along *a* axis in **1** and **2**; (b) The 1D chains of **1** mutually connected along *b* axis through K^+ atoms; (c) The coordination sphere of the K atom in compound **1**; (d) The 1D chains of **2** mutually connected along *b* axis through hydrogen bonds, shown as black dashed lines; (e) Three different bridging modes of the oxalate group observed in **1** and **2**: bis(bidentante) [μ-1,2,3,4], bidentate-monodentate [μ-1,1,2], and bidentate-bis(monodentate) [μ_3-1,2,3,4].

Recently published oxalate-based networks have showed proton conductivity related to the presence of ammonium and/or crystallization water.[2a,5c,5e] However, no signature of

View Article Online
DOI: 10.1039/C9DT01196A

proton conduction was found in **2** (containing NH_4^+) which exhibits rather insulating behavior with a very low electrical conductivity of ≈1.1 × 10^{-14} (Ω cm)$^{-1}$ over a wide temperature range, from 20 to 120 °C (Fig. S5†)

Interestingly and not common for the heterometallic oxalate-bridged systems, in each of these two complexes three different bridging modes of the oxalate ligand are observed (Fig. 1e); CSD[4] search found only a few heterometallic compounds containg transition metals in which oxalate anion adopts two different coordination modes [mostly bis(bidentate) + bidentate-monodentate through terminal oxygen atoms].[2a,6] It appears that slow diffusion and solvent mixture used herein addresses reproducibly the unprecedented bridging modes forming structures with noteworthy characteristics.

The change of *N*-donor aromatic ligand from bpy to phen with the addition of $K_2Cr_2O_7$ in the same reaction mixture influenced notably the reaction outcome. The obtained yellow polyhedra of **3** contain 1D ladder-like [$Cr^{VI}Cu^{II}$] chains, in which copper(II) ions from symmetrical oxalate-bridged [Cu(phen)(μ-C_2O_4)Cu^i(phen)]$^{2+}$ units [symmetry operator: (*i*) = –*x*, –*y*, 1 – *z*] are bridged through oxygen atoms of $Cr_2O_7^{2-}$ anions along *a* axis (Fig. 2). As in compounds **1** and **2**, the oxalate release of [$Cr(C_2O_4)_3$]$^{3-}$ and its delivery allows obtaining cationic species. Compound **3** crystallizes in the $P\overline{1}$ space group and is disordered, so X-ray data were collected at 100(2) K (Fig. S3†). To our knowledge, this type of bridging mode found in compound **3** [μ_4-tetra(monodentate)] has not yet been reported: $Cr_2O_7^{2-}$ bridges four Cu^{2+} ions from two [$Cu_2(phen)_2(\mu$-$C_2O_4)$]$^{2+}$ units through four terminal oxygen atoms in ladder-like mode (Fig. 2).

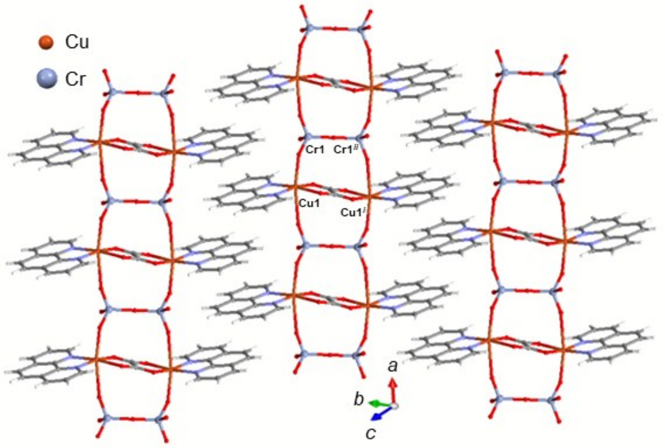

Fig. 2 The 1D ladder-like chains made of [$(Cr_2O_7)Cu_2(C_2O_4)(phen)_2$] units along *a* axis in 3. The aromatic systems of the neighbouring chains are stacked by π-interactions between phen moieties along *a* axis. Symmetry operator: (*i*) = –*x*, –*y*, 1 – *z*, (*ii*) = 1 –*x*, –*y*, 1 – *z*.

Copper(II) ion, beside O atoms from dichromate in apical positions [Cu1–O1 = 2.244(3) Å and Cu1–O4A^{iii} = 2.571(9) Å; symmetry operator: (*iii*) –1 + *x*, *y*, *z*], is coordinated by two N atoms from phen molecule [1.983(4) and 2.005(4) Å] and two O atoms from bridging bis(bidentate) oxalate group [1.978(4) and 1.982(3) Å] (Table S1†). The Cu1···Cu1^i [symmetry operator: (*i*) = –*x*, –*y*, 1 – *z*] distance across the bridging oxalate group is 5.1315(14) Å. The aromatic systems of the neighbouring [$(Cr_2O_7)Cu_2(C_2O_4)(phen)_2$] chains are stacked by *π*-interactions between phen moieties along *a* axis (Fig. 2; Table S3†). The use of $K_2(C_2O_4)\cdot H_2O$ instead of $K_3[Cr(C_2O_4)_3]\cdot 3H_2O$ resulted in a much lower yield and purity of compound **3**, without single-crystals.

Infrared study

The IR spectra of compounds **1** and **2** show characteristic absorption bands of the coordinated [bis(bidentate) and bidentate-bis(monodentate) mode] and uncoordinated [bidentate-monodentate] CO groups of oxalate ligands (Table 1). Beside absorption bands corresponding to the bis(bidentate) bridging oxalate ligands (Table 1), those with a maximum located at 944 and 921 cm^{-1} in the spectra of **3** could be recognized as ν(Cr–O) from dichromate.[14a]

Other absorption bands of the significant intensity in the spectra **1**–**3** correspond to different vibrations of chelating bidentate oxalate groups and coordinated *N*-donor ligands.[15]

Table 1 Selected absorption bands (cm^{-1}) of the oxalate group in the infrared spectra of compounds **1**–**3**

Comp.	*bidentate-monodentate oxalate group*			*bis(bidentate) / bidentate-bis(monodentate) oxalate group*		
	ν_{as}(CO)	ν_s(CO)	*δ(OCO)*	ν_{as}(CO)	ν_s(CO)	*δ(OCO)*
1	1709, 1680	1385	806	1648	1356	781
2	1706, 1675	1383	809	1648	1358	797
3	–	–	–	1642	1348	804

Magnetization study

The temperature dependence of the magnetic susceptibility, $\chi(T)$, for compounds **1**–**3** (Fig. 3) was measured on polycrystalline powder samples in the temperature range 2–290 K in magnetic field of 1000 Oe, as well as the magnetization as a function of applied field, *M(H)*, for several temperatures in the range 2–20 K (Figs. S6–S8†). No magnetic irreversibilities were observed, neither in form of the magnetic hysteresis even at the lowest temperatures (2 and 5 K), nor in form of the splitting between the zero-field cooled (ZFC) and field-cooled (FC) magnetization curves. The *M(H)* curves for **1** and **2** measured at 2 K approach the saturation in high fields (50000 Oe) attaining the molar magnetization of 16000 emu Oe mol^{-1} (2.86 Nμ_B) and 17550 emu Oe mol^{-1} (3.14 Nμ_B), respectively (Figs. S6 and S7†). These values correspond to the expected saturated moment of Cr^{3+} with spin S = 3/2. Therefore, these *M(H)* measurements suggest that copper(II) ions from [Cu(bpy)(μ-C_2O_4)Cu(bpy)]$^{2+}$ cations, mediated via oxalate bridge, in **1** and **2** are coupled antiferromagnetically with very strong interaction. The *M*(*H*) curves are linear up to fields considerably above 1000 Oe, so 1000 Oe was used for *M*(*T*) measurements ensuring linear response.

The $\chi T(T)$ dependences for **1** and **2** have similar behaviour, being not a straight line at high temperatures. Values of the χT at RT is lower than expected for the spin only values for non-interacting two spins 1/2 (Cu^{2+}) and one spin 3/2 (Cr^{3+}). Cooling down $\chi T(T)$ is decreasing and reaches plateau below 50 K

View Article Online
DOI: 10.1039/C9DT01195A

which corresponds to the value expected for Cr^{3+} ion. All this points out strong antiferromagnetic interaction between Cu^{2+} ions bridged by oxalate group, besides the independent paramagnetic Cr^{3+} ions.

In order to extract the magnetic interaction within dimer, magnetic behaviour of **1** and **2** is reproduced by a simple 0-D spin Hamiltonian:

$$\mathrm{H} = -JS_1 \cdot S_2 + D\left(S_{3,z}^2 - \frac{S_3(S_3+1)}{3}\right) + \sum_{i=1}^{3} g_i \mu_B H \cdot S_i \qquad (1),$$

where S_1 and S_2 are spins of Cu^{2+} and S_3 of Cr^{3+}, and other symbols have their usual meaning. The best fitting was obtained for parameters: g_{Cu} = 2.07, g_{Cr} = 2.01, J = –343 cm^{-1}, $|D_{Cr}|$ = 0.15 cm^{-1} for **1** and g_{Cu} = 2.24, g_{Cr} = 2.04, J = –371 cm^{-1}, $|D_{Cr}|$ = 0.05 cm^{-1} for **2**. The J parameters for these compounds obtained with DFT calculations are –382 and –377 cm^{-1}, respectively, supporting the validity of susceptibility modelling. Obtained g-factors are within the absolute accuracy of the instrument in very good agreement with usual values for such ions, as well as D parameters.

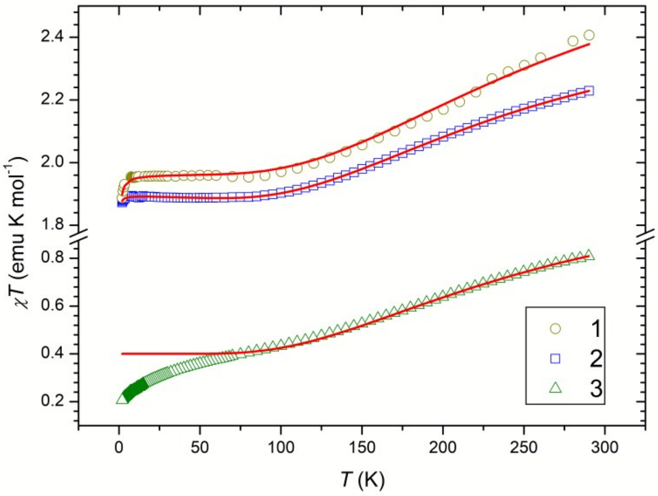

Fig. 3 Temperature dependence of the product χT for compounds **1**–**3**. The red solid lines are model curves. Note the large break on χT axis.

Bending of the $\chi T(T)$ curve for compound **3** at temperatures above 100 K is similar to the behaviour in **1** and **2**, suggesting as well very strong antiferromagnetic interaction between copper(II) centres. In dichromate Cr^{6+} ion is in diamagnetic state, and with cooling down $\chi T(T)$ should gradually reach value of zero. Here the measurements do not show such ideal behaviour, therefore we could not apply fitting of simple model as for **1** and **2**. Therefore, the $\chi T(T)$ curve was simulated using J = –340 cm^{-1} obtained from the DFT calculations, g = 2.14, and paramagnetic susceptibility contribution of 0.4 emu K mol^{-1}. Curve matches the measured data in high temperature region confirming thus the strong antiferromagnetic interaction between Cu^{2+} ions which determines dominantly the curvature of $\chi T(T)$. Since the added paramagnetic contribution in **3** is much smaller than contribution of Cr^{3+} in **1** and **2**, as confirmed also with $M(H)$ measurements, its origin is ascribed to possible magnetic impurities (Fig. 9†).

DFT calculations with doubled cell for all three compounds show that second neighbour magnetic interactions between Cu^{2+} ions are negligible, as well as with Cr^{3+} ions, justifying thus the performed magnetic modelling.

Several structural parameters in oxalate-bridged binuclear copper(II) complexes, such as the Cu···Cu separation across the bridging oxalate, the dihedral angle between the mean oxalate and equatorial planes, or the distance of the copper atom from basal plane, influence the strength of antiferromagnetic interaction.[16] The values of these parameters for compounds **1**–**3** are approximate to those of similar oxalate-bridged copper(II) moieties containing same *N*-ancillary ligands and an entirely planar $[Cu(L)(\mu\text{-}C_2O_4)Cu(L)]$ array (Table S3†).[17] The obtained values of J indicate a maximized antiferromagnetic interaction as a consequence of the 4 + 2 coordination of oxalate-bridged copper(II) centres.

Conclusions

In summary, three 1D heterometallic coordination polymers (CPs) are obtained by diffusion, in which $[\{Cu(L)\}_2(\mu\text{-}C_2O_4)]^{2+}$ cations are bridged by $[Cr(C_2O_4)_3]^{3-}$ (**1** and **2**) or $Cr_2O_7^{2-}$ (**3**). In these two types of compounds, $[Cr(C_2O_4)_3]^{3-}$ and $Cr_2O_7^{2-}$ bridges four copper(II) centers, thus forming novel ladder-like topologies.

These compounds show unique structures due to:

(*i*) the partial decomposition of the tris(oxalato)chromate(III) anion during the crystallization process of **1**–**3**;

(*ii*) so far unknown way of coordination of the $[Cr(C_2O_4)_3]^{3-}$ building block in **1** and **2** – two different bridging modes of the oxalate ligand between Cr^{3+} and Cu^{2+} are observed:[18] μ-1,1,2 [bidentate-monodentate through non-terminal oxygen atom][11,12,] and μ_3-1,2,3,4 [bidentate-bis(monodentate)];[13]

(*iii*) altogether three different observed bridging modes of the oxalate ligand in **1** and **2**;

(*iv*) the extraordinary and novel bridging ladder-like μ_4-tetra(monodentate) mode of $Cr_2O_7^{2-}$ in **3**;[4,19]

(*v*) for the first time $C_2O_4^{2-}$ and $Cr_2O_7^{2-}$ act as bridging ligands in the same compound (**3**).

Magnetic measurements and DFT calculations have shown very strong antiferromagnetic interaction, which couples copper spins into singlet. It has also been demonstrated that the peculiar bridging modes of used building blocks do not create observable magnetic interactions along ladders nor between them.

Experimental

Materials and physical measurements

All chemicals were purchased from commercial sources and used without further purification. The precursor salt $K_3[Cr(C_2O_4)_3]\cdot 3H_2O$ was prepared according to the method described in the literature.[20] The preparation method used for the synthesis of $(NH_4)_3[Cr(C_2O_4)_3]\cdot 3H_2O$ has been derived from those of the potassium salt by replacing the potassium reactants by the ammonium homologues. Elemental analyses for C, H and N were performed with a Perkin–Elmer Model 2400 microanalytical analyzer. Infrared spectra were recorded with KBr pellets using a Bruker Alpha-T spectrometer in the 4000–350 cm^{-1} range.

Synthetic procedures

Synthesis of $\{K[CrCu_2(bpy)_2(C_2O_4)_4]\cdot H_2O\}_n$ (1). An aqueous solution (3 mL) of $K_3[Cr(C_2O_4)_3]\cdot 3H_2O$ (0.049 g; 0.1 mmol) was layered with a mixture of methanol solutions (8 mL) of $CuCl_2\cdot 2H_2O$ (0.017 g; 0.1 mmol) and 2,2'-bipyridine (0.016 g; 0.1 mmol) in a test tube. The blue-green rod-like single crystals of **1** were formed after 7 days, washed with a small amount of water and dried in air. The yield was 58%. Anal. Calcd for $C_{28}H_{18}CrCu_2KN_4O_{17}$ (**1**; *Mr* = 900.64): C, 37.34; H, 2.01; N, 6.22: Found: C, 37.36; H, 2.04; N, 6.25%. IR data (KBr, cm^{-1}): 3452 (s), 1709 (vs), 1680 (vs), 1648 (vs), 1615 (sh), 1499 (w), 1477 (w), 1450 (m), 1385 (m), 1356 (w), 1315 (w), 1254 (w), 1160 (w), 1109 (w), 1059 (w), 1036 (w), 1023 (w), 979 (w), 891 (w), 806 (m), 781 (m), 768 (w), 730 (w), 666 (w), 650 (w), 545 (m), 495 (w), 480 (w), 416 (m).

Synthesis of $\{(NH_4)[CrCu_2(bpy)_2(C_2O_4)_4]\cdot H_2O\}_n$ (2). An aqueous solution (3 mL) of $(NH_4)_3[Cr(C_2O_4)_3]\cdot 3H_2O$ (0.043 g; 0.1 mmol) was layered with a mixture of methanol solutions (8 mL) of $CuCl_2\cdot 2H_2O$ (0.018 g; 0.1 mmol) and 2,2'-bipyridine (0.016 g; 0.1 mmol) in a test tube. The blue-green rod-like single crystals of **2** formed after 7 days, washed with a small amount of water and dried in air. The yield was 52%. Anal. Calcd for $C_{28}H_{22}CrCu_2N_5O_{17}$ (**2**; *Mr* = 879.58): C, 38.23; H, 2.52; N, 7.96: Found: C, 38.26; H, 2.54; N, 7.98%. IR data (KBr, cm^{-1}): 3437 (s), 1706 (vs), 1675 (vs), 1648 (sh), 1617 (s), 1574 (w), 1501 (w), 1478 (w), 1450 (m), 1383 (m), 1358 (w), 1318 (w), 1252 (w), 1161 (w), 1107 (w), 1060 (w), 1036 (w), 1023 (w), 977 (w), 893 (w), 809 (m), 797 (sh), 768 (w), 731 (w), 667 (w), 650 (w), 548 (m), 495 (w), 468 (w), 419 (m).

Synthesis of $[(Cr_2O_7)Cu_2(C_2O_4)(phen)_2]_n$ (3). An aqueous solution (4 mL) containing $K_3[Cr(C_2O_4)_3]\cdot 3H_2O$ (0.026 g; 0.05 mmol) and $K_2Cr_2O_7$ (0.016 g; 0.05 mmol) was layered with a methanol solution (8 mL) of $CuCl_2\cdot 2H_2O$ (0.018 g; 0.1 mmol) and 1,10-phenanthroline (0.021 g; 0.1 mmol) in a test tube. Yellow prismatic single crystals of **3** formed after few days, were washed with a small amount of water and dried in air. The yield was 21 %. Anal. Calcd for $C_{13}H_8CrCuN_2O_{5.5}$ (**3**; Mr = 395.75): C, 39.45; H, 2.04; N, 7.08: Found: C, 39.47; H, 2.10; N, 7.05%. IR data (KBr, cm–1): 3440 (w), 1642 (vs), 1518 (w), 1492 (w), 1427 (m), 1385 (m), 1348 (m), 1308 (w), 1222 (w), 1151 (w), 1111 (w), 1050 (w), 1032 (w), 944 (s), 921 (s), 878 (w), 845 (w), 804 (m), 770 (w), 720 (m), 477 (w), 433 (w).

Single-crystal X-ray structural study

X-ray data for single crystals of compounds **1**–**3** were collected by ω-scans on an Oxford Diffraction Xcalibur Nova R diffractometer with mirror-monochromated Cu-Kα radiation (λ = 1.54179 Å, microfocus tube, CCD detector), for **1** and **2** at 293(2) K, while that of **3** at 108(2) K. The crystal data and details of data collections and refinements for the structures reported are summarized in Table 2. Data reduction, including the multi-scan absorption correction, was performed by the CrysAlisPRO software package.[21] The solution, refinement and analysis of the structures were performed using the programs integrated in the WinGX system.[22] The structures were solved by direct methods (SIR92)[23] and refined by the full-matrix least-squares method based on F^2 against all reflections (SHELXL-2017/1).[24] All non-hydrogen atoms were refined anisotropically. The hydrogen atoms attached to the carbon atoms of aromatic ligands were treated as riding entities in idealized positions, with the C–H distances of 0.93 Å and displacement parameters assigned $U_{iso}(H) = 1.2U_{eq}(C)$. The geometry of the water molecules as well as of the ammonium cation was constrained to $d(O/N–H) = 0.95(2)$ Å and $d(H\cdots H) = 1.50(4)$ Å. Displacement parameters of all water hydrogen atoms were assigned as $U_{iso}(H) = 1.5U_{eq}(O)$. Dichromate moieties in **3** are disordered with two positions of non-coordinated oxygen atoms (Fig. S3†). These could not be properly resolved at room temperature, so the data were collected at 108(2) K. Geometrical calculations were carried out with PLATON[25] and the figures were made by the use of the CCDC-Mercury,[26] ORTEP-3,[22] VESTA[27] and ToposPro[28] programs.

Electrical characterization

Electrical conductivity of compound **2** in the form of a pressed pellet was measured by impedance spectroscopy (Novocontrol Alpha-N dielectric analyzer) in the frequency range 0.01 Hz–1 MHz from 20 °C to 120 °C. For the electrical contacts, gold electrodes (3.8 mm in diameter) were sputtered on the opposite surfaces of the pellet. The impedance spectra were analysed by equivalent circuit modelling using the complex nonlinear least-squares fitting procedure (*ZView* software).

The experimental complex impedance at 20 °C of compound **2** exhibits an arc at high values of impedance indicating low electrical conductivity, Fig. S5†. Such impedance data can be well approximated by the equivalent electrical circuit consisting of a parallel combination of resistor and capacitor. The parameters of the equivalent circuit, i.e. electrical resistance (*R*) and capacitance (*C*), obtained by the complex non-linear least squares fitting are shown in Fig. S5†. From the values of electrical resistance (*R*) and electrode dimensions (*A* is the electrode area and *d* is the sample thickness) DC conductivity is calculated according to relation: $\sigma_{DC} = d/(A\cdot R)$. The value of electrical conductivity of compound **2** at 20 °C is 1.1×10^{-14} $(\Omega\ \mathrm{cm})^{-1}$. With increasing temperature up to 120 °C the impedance spectra remains nearly the same revealing that conductivity of **2** is very weakly temperature dependent. This further suggests the absence of proton transfer in the conduction process in compound **2**.

Magnetization study

The magnetization *M* of a polycrystalline samples was measured with an MPMS 5 commercial superconducting quantum interferometer device (SQUID) magnetometer. The measured magnetic moments of the samples were corrected by taking into account the sample holder, temperature-independent contributions of the core electrons in accordance with the well-known Pascal constants and temperature independent paramagnetic contribution of copper(II). Calculations of numerical fits and simulations were performed using own developed program in Python.

DFT calculations

The plane-wave DFT code Quantum ESPRESSO14,[29,30] with GBRV pseudopotentials[31] was used to study magnetic properties of the compounds **1**–**3**. The energy cut-off for the plane wave basis set is set to 680 eV. Relaxation of ionic positions starting from experimental structures was performed until forces on all atoms were smaller than 0.01 eV Å^{-1} and change in energy of two consecutive steps was smaller than 0.5 meV. The Brillouin zone is sampled with a Monkhorst-Pack mesh with density of k-points of at least 2 Å. We use PBE[32] exchange correlation functional with +*U* approach[33] to better describe localized *d*-electrons. Parameter U = 10.15 eV is calculated from linear response scheme (see Ref. 33) for compound **3**, and used as such also for **1** and **2**. Magnetic interaction parameters *J* are calculated from differences of total energies of ferromagnetic and antiferromagnetic configurations.

Acknowledgements

This work has been supported by the Croatian Science Foundation under Project Nos. IP-2014-09-4079 and UIP-2014-09-8276.

Notes and references

1 M. Clemente-León, E. Coronado, C. Martí-Gastaldoz and F. M. Romero, *Chem. Soc. Rev.*, 2011, **40**, 473–497.

2. (a) C. Maxim, S. Ferlay, H. Tokoro, S.-I.Ohkoshi and C. Train, *Chem. Commun.*, 2014, **50**, 5629–5632; (b) M. Clemente-León, E. Coronado, C. J. Gómez-García, M. López-Jordà, A. Camón, A. Repollés and F. Luis, *Chem.–Eur. J.*, 2014, **20**, 1669–1676; J. Habjanič, M. Jurić, J. Popović, K. Molčanov and D. Pajić, *Inorg. Chem.*, 2014, **53**, 9633–9643; M. Jurić, D. Pajić, D. Žilić, B. Rakvin, K. Molčanov and J. Popović, *Dalton Trans.*, 2015, **44**, 20626–20635.

3 G. Marinescu, M. Andruh, F. Lloret and M. Julve, *Coor. Chem. Rev.*, 2011, **255**, 161–185.

4 C. R. Groom, I. J. Bruno, M. P. Lightfoot and S. C. Ward, *Acta Crystallogr., Sect. B: Struct. Sci., Cryst. Eng. Mater.*, 2016, **B72**, 171–179.

5 (a) E. Pardo, C. Train, H. Liu, L.-M. Chamoreau, B. Dkhil, K. Boubekeur, F. Lloret, K. Nakatani, H. Tokoro, S.-i. Ohkoshi and M.Verdaguer, *Angew. Chem. Int. Ed.,* 2012, **51**, 8356–8360; (b) E. Pardo, C. Train, K. Boubekeur, G. Gontard, J. Cano, F. Lloret, K. Nakatani and M. Verdaguer, *Inorg. Chem.*, 2012, **51**, 11582 11593; (c) E. Pardo, C. Train, G. Gontard, K. Boubekeur, O. Fabelo, H. Liu, B. Dkhil, F. Lloret, K. Nakagawa, H. Tokoro, S.-i. Ohkoshi and M. Verdaguer, *J. Am. Chem. Soc.*, 2011, **133**, 15328-15331; (d) M. Jurić, P. Planinić, N. Brničević, D. Milić, D. Matković-Čalogović, D. Pajić K. Zadro, *Eur. J. Inorg. Chem.* 2006, 2701–2710; (e) H. Ōkawa, A. Shigematsu, M. Sadakiyo, T. Miyagawa, Ko Yoneda, M. Ohba and H. Kitagawa, *J. Am. Chem. Soc.*, 2009, **131**, 13516–13522.

6 (a) E. Coronado, J. R. GalánMascarós and C. Martí-Gastaldo, *Inorg. Chim. Acta*, 2008, **361**, 4017–4023; (b) H.-Z. Kou, and O. Sato, *Inorg. Chem.*, 2007, **46**, 9513-9515; (c) Y. Miyazato, M. Ohba, H. Ōkawa, *Bull. Chem. Soc. Jpn.*, 2005, **78**, 1646–1648; (d) A. Alberola, E. Coronado, C. Giménez-Saiz, C. J. Gómez-García, F. M. Romero and Ana Tarazón, *Eur. J. Inorg. Chem.*, 2005, 389–400; (e) G. Ballester, E. Coronado, C. Giménez-Saiz and F. M. Romero, *Angew. Chem. Int. Ed.*, 2001, **40**, 792-795; (f) O. Costisor, K. Mereiter, M. Julve, F. Lloret, Y. Journaux, W. Linert and M. Andruh, *Inorg. Chim. Acta*, 2001, **324**, 352–358.

7 (a) H. S. Scott, A. Bajpai, K.-J. Chen, T. Pham, B. Space, J. J. Perry IV and M. J. Zaworotko, *Chem. Commun.*, 2015, **51**, 14832–14835; (b) A. L. Kopf, P. A. Maggard, C. L. Stern and K. R. Poeppelmeier, *Acta Crystallogr.*, 2005, **C61**, m165–m168; (c) L. Pan, N. Ching, X. Huang and J. Li, *Chem. Commun.*, 2001, 1064–1065; (d) A. J. Norquist, K. R. Heier, P. S. Halasyamani, C. L. Stern, K. R. Poeppelmeier, *Inorg. Chem.*, 2001, **40***,* 2015–2019.

8 (a) R. Karmakar, C. R. Choudhury, V. Gramlich and S. Mitra, *Inorg. Chim. Acta*, 2004, **357**, 3785–3788; (b) Y. Hayashi, T. Tagami, H. Mano and A. Uehara, *Chem. Lett.* 2001, 562–563; (c) L. Pan, N. Zheng, X. Zhou, Y. Wu, Q. Wu and X. Jin, *Acta Crystallogr.*, 1998, **C54**, 1802–1804; (d) Y. Hayashi, H. Mano and A. Uehara, *Chem. Lett.*, 1998, 899–900.

9 (a) X.-Y. Chen, B. Zhao, P. Cheng, B. Ding, D.-Z. Liao,S.-P.Yan and Z.-H.Jiang, *Eur. J. Inorg. Chem.*, 2004, 562–569; (b) G. De Munno, T. Poerio, M. Julve, F. Lloret and J. Faus, *J. Chem. Soc.*, *Dalton Trans.*, 1998, 1679–1685; (c) B. C. Dave and R. S. Czernuszewicz, *Inorg. Chem.*, 1994, **33**, 847–848. (d) B. Jameson, N. Seferiadis and R. Oswald, *Acta Crystallogr.*, 1986, **C42**, 984–987.

10 (a) L. Androš Dubraja, M. Jurić, F. Torić and D. Pajić, *Dalton Trans.*, 2017, **46**, 11748–11756; (b) W. X. C. Oliveira, C. L. M. Pereira, C. B. Pinheiro, F. Lloret and M. Julve, *Inorg. Chem. Front.*, 2018, **5**, 1294–1306; (c) W. X. C. Oliveira, C. L. M. Pereira, C. B. Pinheiro, F. Lloret and M. Julve, *J. Coord. Chem.*, 2018, **71**, 707–724.

11 (a) Z.-H. Dang, J. Zhao and L.Xu, *Inorg. Chim. Acta,* 2009, **362**, 2999–3004; (b) K. Kadir, T. M. Ahmed, D. Noreús and L. Eriksson, *Acta Crystallogr.,* 2006, **E62**, m1139–m1141; (c) J. P. García-Terán, O. Castillo, A. Luque, U. García-Couceiro, G. Beobide and P. Román, *Dalton Trans.,* 2006, 902– 911; (d) S. K. Chattopadhyay, T. C. W. Mak, B.-S. Luo, L. K. Thompson, A. Rana and S. Ghosh, *Polyhedron*, 1995, **14**, 3661–3667; (d) U. Geiser, B. L. Ramakrishna, R. D. Willett, F. B. Hulsbergen and J. Reedijk, *Inorg. Chem.,* 1987, **26***,* 3750–3756; (e) Y. Pongchan, P. E. Nixon, J. M. Waters and T. N. Waters, *Acta Crystallogr.,* 1980, **B36**, 2145–2147; (f) A. Gleizes, F. Maury and J. Galy, *Inorg. Chem.,* 1980, **19**, 2014–2018.

12 (a) E. N. Chygorin, V. G. Makhankova, V. N. Kokozay, V. V. Dyakonenko, O. V. Shishkin and J. Jezierska, *Inorg. Chem. Commun*., 2010, **1**, 1509–1511; (b) F. R.Y. Louka, F. A. Mautner, R. Vicente and S. S. Massoud, *Inorg. Chem. Commun.*, 2008, **11**, 438–441; (c) M.-L. Zhu, *Acta Crystallogr.*, 2006, **E62**, m1985–m1987; (d) T. D. Keene, M. B. Hursthouse, D. J. Price, *Acta Crystallogr.*, 2004, **E60**, m378–m380; (e) M. Hernández-Molina, P. A. Lorenzo-Luis and C. Ruiz-Pérez, *CrystEngComm*, 2001, **3**, 60–63; (f) M. Andruh, R. Melanson, C. V. Stager and F. D. Rochon, *Inorg. Chim. Acta*, 1996, **251**, 309–317.

13 (a) J.-H. Li, H. Liu, L. Wei and G.-M. Wang, *Solid State Sci.*, 2015, **48**, 225–229; (b) R. Vaidhyanathan, S. Neeraj, P.A. Prasad, Srinivasan Natarajan and C.N.R. Rao, *Angew. Chem. Int. Ed.,* 2000, **39**, 3470–3473; (c) X. Yang, J. Li, Y. Hou, S. Shi and Y. Shan, *Inorg. Chim. Acta*, 2008, **361**, 1510–1514; (d) H. Liu, W. Gu, G. Xu, Y. Feng, Y. Kou, L. Feng, S. Yan, D. Liao and P. Cheng, *Inorg. Chem. Commun.*, 2007, **10**, 1099–1101; (e)

View Article Online
DOI: 10.1039/C9DT01195A

R. Vaidhyanathan, S. Natarajan and C. N. R. Rao, *Chem. Mater.*, **2001**, *13,* 3524–3533.
14 B. Cordero, V. Gómez, A. E. Platero-Prats, M. Revés, J. Echeverría, E. Cremades, F. Barragán and S. Alvares, *Dalton Trans.*, 2008, 2832–2838.
15 K. Nakamoto, *Infrared and Raman Spectra of Inorganic and Coordination Compounds*, John Wiley, New York, 6th edn, 2009.
16 M. J. Belousoff, B. Graham, B Moubaraki, K. S. Murray and L. Spiccia, *Eur. J. Inorg. Chem.*, 2006, 4872–4878.
17 (a) O. Castillo, I. Muga, A. Luque, J. M. Gutiérrez-Zorrilla, J. Sertucha, P. Vitoria and P. Román, *Polyhedron*, 1999, **18**, 1235–1245; (b) M. Julve, J. Faus, M. Verdaguer and A. Gleizes, *J. Am. Chem. Soc.*, 1984, **106**, 8306–8308; (c) A. Gleizes, M. Julve, M. Verdaguer, J. A. Real, J. Faus and X. Solans, *J. Chem. Soc., Dalton Trans.*, 1992, 3209–3216; (d) A. Bencini, A. C. Fabretti, C. Zanchini and P. Zannini, *Inorg. Chem.*, 1987, **26**, 1445–1449; (e) M. Jurić, D. Pajić, Dijana Žilić, B. Rakvin, D. Milić and P. Planinić, *Polyhedron*, 2015, **98**, 26–34.
18 (a) O. Castillo, A. Luque, S. Iglesias, C. Guzmán-Miralles and P. Román, *Inorg. Chem. Commun*, 2001, **4**, 640–642: (b) H. Núñez, J.-J. Timor, J. Server-Carrió, L. Soto and E. Escrivà, *Inorg. Chim. Acta*, 2001, **318**, 8–14; (d) A. Świtlicka-Olszewska, B. Machura, J. Mroziński, B. Kalińka, R. Kruszynski and M. Penkala, *New J. Chem.,* 2014, **38**, 1611—1626.
19 (a) V. Kulikov and G. Meyer, Cryst. Growth Des., 2013, **13**, 2916–2927; (b) A. Beheshti, H. R. Zafarian, R. Khorramdin, M. Fattahi Monavvar and C. T. Abrahams, *Polyhedron*, 2012, **48**, 245–252.
20 G. Brauer (Ed.), *Handbuch der Präparative Anorganischen Chemie*, Ferdinand Enke Verlag, Stuttgart, 1954.
21 Agilent. CrysAlis PRO, Agilent Technologies Ltd, Yarnton, England, 2014.
22 L. J. Farrugia, *J. Appl. Crystallogr.*, 2012, **45**, 849–854.
23 A. Altomare, G. Cascarano, C. Giacovazzo, A. Guagliardi, M. C. Burla, G. Polidori and M. Camalli, *J. Appl. Crystallogr.*, 1994, **27**, 435.
24 G. M. Sheldrick, *Acta Crystallogr., Sect. A: Found. Adv.*, 2015, **71**, 3–8.
25 A. L. Spek, *Acta Crystallogr., Sect. D: Biol. Crystallogr.*, 2009, **65**, 148–155.
26 C. F. Macrae, P. R. Edgington, P. McCabe, E. Pidcock, G. P. Shields, R. Taylor, M. Towler and J. van de Streek, *J. Appl. Crystallogr.*, 2006, **39**, 453–457.
27 K. Momma and F. Izumi, *J. Appl. Crystallogr.*, 2011, **44**, 1272–1276.
28 V. A. Blatov, *Crystallogr. Rev.*, 2004, **10**, 249–318.
29 P. Giannozzi, S. Baroni, N. Bonini, M. Calandra, R. Car, C. Cavazzoni, D. Ceresoli, G. L. Chiarotti, M. Cococcioni, I. Dabo, A. Dal Corso, S. de Gironcoli, S. Fabris, G. Fratesi, R. Gebauer, U. Gerstmann, C. Gougoussis, A. Kokalj, M. Lazzeri, L. Martin-Samos, N. Marzari, F. Mauri, R. Mazzarello, S. Paolini, A. Pasquarello, L. Paulatto, C. Sbraccia, S. Scandolo, G. Sclauzero, A. P. Seitsonen, A. Smogunov, P. Umari andR. M. Wentzcovitch, *J. Phys.: Condens. Matter*, 2009, **21**, 395502.
30 P. Giannozzi, O. Andreussi, T. Brumme, O. Bunau, M. Buongiorno Nardelli, M. Calandra, R. Car, C. Cavazzoni, D. Ceresoli, M. Cococcioni, N. Colonna, I. Carnimeo, A. Dal Corso, S. de Gironcoli, P. Delugas, R. A. DiStasio Jr, A. Ferretti, A. Floris, G. Fratesi, G. Fugallo, R. Gebauer, U. Gerstmann, F. Giustino, T. Gorni, J. Jia, M. Kawamura, H.-Y. Ko, A. Kokalj, E. Küçükbenli, M. Lazzeri, M. Marsili, N. Marzari, F. Mauri, N. L. Nguyen, H.-V. Nguyen, A. Otero-de-la-Roza, L. Paulatto, S. Poncé, D. Rocca, R. Sabatini, B. Santra , M. Schlipf, A. P. Seitsonen, A. Smogunov, I. Timrov, T. Thonhauser, P. Umari, N. Vast, X. Wu and S. Baroni, *J. Phys.: Condens. Matter*, 2017, 29, 465901.
31 K. F. Garrity, J. W. Bennett, K. M. Rabe and D. Vanderbilt, *Comput. Mater. Sci.*, 2014, **81**, 446–452.
32 J. P. Perdew, K. Burke and M. Ernzerhof, *Phys. Rev. Lett.*, 1996, **77**, 3865–3868.
33 M. Cococcioni and S. de Gironcoli, *Phys. Rev. B*, 2005, **71**, 035105.

Table 2 Crystallographic data and structure refinement details for compounds $\{K[CrCu_2(bpy)_2(C_2O_4)_4]\cdot H_2O\}_n$ (**1**), $\{(NH_4)[CrCu_2(bpy)_2(C_2O_4)_4]\cdot H_2O\}_n$ (**2**) and $[(Cr_2O_7)Cu_2(C_2O_4)(phen)_2]_n$ (**3**)

Compound	**1**	**2**	**3**
empirical formula	$C_{28}H_{18}CrCu_2KN_4O_{17}$	$C_{28}H_{22}CrCu_2N_5O_{17}$	$C_{13}H_8CrCuN_2O_{5.5}$
crystal colour, habit	Blue-green, rod	Blue-green, rod	Yellow, prism
fw (g mol^{-1})	900.64	879.58	395.75
crystal dimensions (mm)	0.30 × 0.07 × 0.03	0.40 × 0.05 × 0.04	0.12 × 0.04 × 0.02
T (K)	293(2)	293(2)	108(2)
Space group	$P\bar{1}$	$P\bar{1}$	$P\bar{1}$
a (Å)]	7.802(5)	7.8102(2)	7.2322(6)
b (Å)	9.601(5)	9.8600(4)	9.7882(8)
c (Å)	21.566(5)	21.4368(9)	10.0034(6)
α (deg)	80.760(5)	80.494(3)	91.630(6)
β (deg)	88.103(5)	88.882(3)	109.709(7)
γ (deg)	82.201(5)	81.638(3)	95.890(7)
V (Å^3)	1579.6(14)	1610.82(10)	661.63(9)
Z	2	2	2
$D_{calc.}$ (g cm^{-3})	1.894	1.813	1.986
μ (mm^{-1})	6.334	5.066	9.057
F(000)	902	886	394
Θ range (deg)	4.15–82.31	4.18–76.00	4.552–76.090
Diffractometer type	Xcalibur Nova R	Xcalibur Nova R	Xcalibur Nova R
h, k, l range	$-6 < h < 9$; $-11 < h < 12$; $-26 < h < 26$	$-4 < h < 9$; $-12 < h < 12$; $-26 < h < 26$	$-9 < h < 6$; $-12 < h < 12$; $-9 < h < 12$
no. of measured reflections	14627	13929	4683
no. of independent reflections	6459	6574	2593
No. of observed reflections	5424	6120	2144
R_{int}	0.0612	0.0305	0.0597

View Article Online
DOI: 10.1039/C9DT01195A

R, *wR* [$I > 2\sigma(I)$]	0.0616, 0.1621	0.0430, 0.1245	0.0619, 0.1638
R, wR [all data]	0.0755, 0.1741	0.0454, 0.1205	0.0721, 0.1772
goodness-of-fit	1.043	1.079	1.059
absorption correction	multi-scan	multi-scan	multi-scan
no. of parameters, restraints	481, 0	502, 13	217, 14
H atom treatment	mixed	mixed	constrained
$\Delta\rho_{max}$, $\Delta\rho_{min}$ (e Å^{-3})	0.691, –0.916	0.664, –0.578	1.225, –1.079